IJREAT International Journal of Research in Engineering & Advanced Technology, Volume 3, Issue 6, Dec -Jan, 2016
ISSN: 2320 – 8791 (Impact Factor: 2.317)
www.ijreat.org

Uncertainty Based On Analyses And Optimal Design Of A Solar Cell

Hoe-Gil Lee[1], Singiresu S. Rao[2]

[1]Assistant Professor, Department of Mechanical Engineering Shiv Nadar University
NH-91, Teshsil Dadri, District Gautam Buddha Nagar U.P. 2101 314, India

[2]Professor, Department of Mechanical and Aerospace Engineering University of Miami,
Coral Gables, FL 33146, USA

Abstract

The aim of uncertainty analysis is to predict the performance of a solar cell in the presence of uncertain parameters. In probabilistic analysis, the random variables of a solar cell include geometric design variables (except for integer values) and uncertain design parameters of top metallic contact. The solar cell have been investigated by varying the values of the weight of mean and coefficient variations and illustrations by applying the parametric study related to the probabilistic efficiency of a solar cell. The fuzzy membership functions are used for modeling the uncertain or imprecise design parameters of a solar cell. Triangular membership functions are used to represent the uncertain parameters as fuzzy quantities. Fuzzy arithmetic operations and extension principles are used for finding the membership functions of the fuzzy response parameters of the system. The deviations of solar cell performance of the conversion efficiency from the crisp value are investigated by varying α-cut interval levels and uncertain input parameters of different fuzzy confidence intervals.

Keywords: Solar cell, Uncertainty, Probabilistic optimization, Fuzzy analysis, Membership function, Geometric design, Genetic Algorithms (GA)

1. Introduction

The purpose of uncertainty analysis is to be able to predict the performance of a solar cell more realistically through the quantification of uncertainties associated with various parameters. In this work, first the uncertainty analysis is investigated using stochastic (or probabilistic) and fuzzy approaches, and then the optimal design of a solar cell is explored through probabilistic and fuzzy analyses. Stochastic or probabilistic methods assume that the parameters of the problem are random variables with known probability distribution. Therefore, stochastic or probabilistic optimization methods involve random variables and, hence, the objective functions and constraints are also random variables. Random variables include uncertain design variables and/or uncertain design parameters or data. The stochastic techniques generate better results as compared to deterministic ones, and the optimal set of design and random variables are a means to produce maximum system performance. This study includes a review of stochastic optimization techniques implemented in finding the prediction of the performance of a solar cell. The geometric parameters are imprecise due to geometric dimensioning and tolerancing from machining settings during production and operator's error, assembling a product, and operating a system. The geometric values used in the optimal design are imprecise as a result of unpredictable engineering environments. Fuzzy sets include some degrees of membership that permit the gradual assessment of the membership of elements in a set.

Arturo [1] calculated the conversion efficiency of a solar cell under concentrated sunlight. Power losses can be divided into two sections: optical and electrical losses in a solar cell. Optical losses are caused by the reflection of solar energy, which can be reduced by antireflection (AR) coating and shadowing of the sunlight. This results in metal grid contact on the side of the cell exposed to sunlight as well as inadequate

absorption of solar radiation, which, if not thick enough, prevents some light from passing through the solar cell. Electrical losses have an influence on resistance from front contact materials and recombination losses. To analyze the performance of solar conversion efficiency, Rault [2] investigated the generation of an electron–hole pair to be probabilistically distributed. It is a given that quantum mechanics is probability-based. The key is which probability distribution functions (PDF) and cumulative distribution function (CDF) best fits the physical mechanics of recombination at the sub-atomic level. There are a number of possible distributions, but overall the one that seems to fit best is the Burr distribution. This approach is to determine radiative lifetime, and the results are compared to an existing device. Hengsritawat [3] investigated a probabilistic approach to desiging an optimal-sized photovoltaic model in a distribution system. In this paper, the objective of the proposed technique is to minimize average system active power losses while considering power quality constraints, such as voltage and current under probability density of solar radiation, power, and voltage as random variables with normal distribution. Thus, the I-V characteristics of PV models are studied to determine the optimal size of a PV model. Zulkifli [4] claimed that PV output is dependent on the solar radiation intermittency and the location of installation. A solar photovoltaic system was analyzed under probabilistic distribution function of the hourly solar radiation in between two different locations in order to analyze I-V characteristics and evaluate solar photovoltaic power systems.

The fuzzy set theory was introduced by Zadeh (1965). Nowadays, this theory is being applied to countless fields within and beyond the scope of conventional engineering. Bellman amd Zadeh [5] extended fuzzy set theory to the fuzzy set-based optimization with decision-making in a fuzzy environment. Xiong and Rao[6] presented fuzzy nonlinear programming for mixed-discrete design optimization through hybrid

genetic algorithms. They proposed a mixed-discrete fuzzy nonlinear programming approach that combines the fuzzy λ-formulation with a hybrid genetic algorithm using mathematical techniques for finding the minimum cost design of a welded beam. Eman [7] investigated a fuzzy approach for a bi-level integer non-linear programming problem (BLI-NLP) which consists of the higher-level decision-maker (HLDM) and the lower-level decision-maker (LLDM). The paper was focused on two planner integer models and a solution method for solving the problem using the concept of tolerance membership function and a set of Pareto optimal solutions. Liang [8] studied fuzzy multi-objective production/distribution planning decisions with multi-product and multi-time period in a supply chain. The paper was focused on a fuzzy multi-objective programming model (FMOLP) with linear membership function to solve integrated multi-product and multi-time period production/distribution planning decision (PDPD) problems with fuzzy objectives.

Stochastic or probabilistic optimization treats the problem that, within the data, is known only as a probability. Therefore, stochastic or probabilistic optimization methods generate and use random variables involving random objective functions or constraints. Random variables contain design variables and/or uncertain design variables. Assumptions about the objective function are probabilistic so that objective and constraint functions depend on optimization variables and random variables. Also, probabilistic sensitivity analysis seeks the rate of change between input and output in solar cells under uncertainties in probabilistic variables of the objective function. To solve the probabilistic optimization problem and conduct the sensitivity analysis given in the conversion efficiency, random variables are adjusted and obtained. Fuzzy set analysis is the membership function in a set assessed in binary terms according to a bivalent condition with membership function values between 0 (an implication of complete comfort) and

1 (an implication of discomfort). The fuzzy set can provide solutions to a broad range of engineering problems. The membership function values indicate the degrees to which each object is compatible with the properties or features distinctive to the collection. The uncertainty in individual measurements of membership function is represented using simple triangular fuzzy numbers.

The purpose is to predict the performance of solar cell in the presence of uncertain parameters and/or to parametric design factors by considering probabilistic and fuzzy analysis methodologies.

2. Probabilistic analysis

2.1 Probabilistic programing form

Stochastic nonlinear programming deals with a general optimization problem with an objective f($\vec{X}$) and /or inequality constraints $g_j(\vec{X})$; j = 1 to m, where, at least one of the functions among f($\vec{X}$) and $g_j(\vec{X})$ is nonlinear in terms of $\vec{X}$ and some of the design variables and/or preassigned parameters are random variables. For simplicity, we assume that all the random variables are independent and follow normal distribution defined in terms of their respective mean values and standard deviations. A probabilistic or stochastic programming problem can be stated as

Find $\vec{X}$ which minimizes f$(\vec{Y})$

subject to

$$P[g_j \leq 0] \geq p_j, \quad j = 1,2,\dots,m \tag{1}$$

where $\vec{Y}$ is the vector of N random variables $y_1, y_2, \ldots, y_N$ that might include the decision variable $x_1, x_2, \ldots, x_l$. Eq. (1) indicates that the probability of realizing $g_j(\vec{Y})$ smaller than or equal to zero must be greater than or equal to the specified probability p_j. The random variables include design parameters except integer values, such as the number of fingers (N_f), busbars (N_b), and concentrated sunlight (C), and uncertain design parameters affecting the results of the objective function. Therefore, the random variables consist of 7 and 8 design parameters and all 4 uncertain design parameters, which include contact resistance (R_c), sheet resistance (R_{sh}), metal resistivity (ρ_m) and incident power (P_{in}) in a square and a rectangular cell, respectively. The solar constant is the rate of total solar energy at all wavelengths incident on a unit area normally exposed to the rays of the sun.

2.2 Objective function

In nonlinear stochastic programming, the objective function contains the uncertainty that depends on a set of random variables based on normal distribution. Thus, the objective function $f(\vec{Y})$ can be expanded as utilizing the mean values of y_i, $\overline{y_l}$, as

$$f(\vec{Y}) = f\left(\vec{\bar{Y}}\right) + \sum_{i=1}^{N}\left(\frac{\partial f}{\partial y_i}\middle|\vec{\bar{Y}}\right)(y_i - \overline{y_l}) + \text{higher} - \text{order derivative terms} \quad (2)$$

If the standard deviations of $y_i$and σ_{yi} are small, $f\left(\vec{Y}\right)$ can be approximated by the first two terms as:

$$f\left(\vec{Y}\right) \cong f(\bar{Y}) - \sum_{i=1}^{N}\left(\left(\frac{\partial f}{\partial y_i}\middle|\vec{\bar{Y}}\right)y_i\right) + \sum_{i=1}^{N}\left(\left(\frac{\partial f}{\partial y_i}\middle|\vec{\bar{Y}}\right)y_i\right) = \psi(Y) \quad (3)$$

If all $y_i(i = 1,2,\ldots,N)$ follow normal distribution, $\psi(Y)$, a linear function of Y, also follows normal distribution. The mean and the variance of ψ are given by

$$\bar{\psi} = \psi\left(\bar{\vec{Y}}\right) \tag{4}$$

$$\mathrm{Var}(\psi) = \sigma_{\psi}^{2} = \sum_{i=1}^{N}\left(\frac{\partial f}{\partial y_i}\middle|\bar{\vec{Y}}\right)^{2}\sigma_{y_i}^{2} \tag{5}$$

since all y_i are independent. For the purpose of optimization, a new objective function $f(\vec{Y})$ can be expressed as

$$f(Y) = k_1\bar{\psi} + k_2\sigma_{\psi} \tag{6}$$

where $k_1 \geq 0$ and $k_2 \geq 0$, and the numerical values of k_1 and k_2 include the important relationship of normal distribution (ψ) standard deviation (σ_{ψ}) for optimization.

2.3 Constraints

Probabilistic constraints contain both decision variables and probabilistic variables, and these follow a probability distribution. The constraints will be probabilistic and one would like to have the probability that a given constraint is satisfied when it is greater than a certain value. The constraint inequality can be written as

$$\int_{-\infty}^{0} f_{gj}(g_j)dg_j \geq \int_{-\infty}^{z_1} f_z(z)d_z = p_j \tag{7}$$

where $f_{gj}(g_j)$ is the probability density function of the random variable, g_j, its range is assumed to be $-\infty$ to ∞. The constraint function $g_j(\vec{Y})$ can be expanded around the vector of mean values of the random variables, $\bar{\vec{Y}}$, as

$$g_j(\vec{Y}) \cong g_j\left(\vec{\bar{Y}}\right) + \sum_{i-1}^{N}\left(\frac{\partial g_j}{\partial y_i}\middle|\vec{\bar{Y}}\right)(y_i - \bar{y_i}) \tag{8}$$

From Eq. (8), the mean value, $\overline{g_j}$, and the standard deviation, σ_{gj}, of g_j can be obtained as

$$\left(\frac{(g_j - \overline{g_j})}{\sigma_{g_j}}\right) > z_1 \tag{9}$$

$$g_j - \overline{g_j} - z_1\sigma_{g_j} \geq 0 \tag{10}$$

$$g_j = 0, \text{ thus } \overline{g_j} + z_1\sigma_{g_j} \leq 0 \tag{11}$$

$$\overline{g_J} = g_j\left(\vec{\bar{Y}}\right) \tag{12}$$

$$\overline{g_J} - \emptyset_j(p_j)\left[\sum_{i=1}^{N}\left(\frac{\partial g_j}{\partial y_i}\middle|\vec{\bar{Y}}\right)^2 {\sigma_{yi}}^2\right]^{1/2} \geq 0 \qquad j = 1,2, \ldots, \text{m} \tag{13}$$

By introducing the new variable

$$\theta = \frac{g_j - \overline{g_j}}{\sigma_{g_j}} \tag{14}$$

and noting that

$$\int_{-\infty}^{\infty} \frac{1}{\sqrt{2\pi}} e^{\frac{-t^2}{2}} dt = 1 \tag{15}$$

Eq. (7) can be rewritten as

$$\int_{-\frac{\overline{g_j}}{\sigma_{g_j}}}^{\infty} \frac{1}{\sqrt{2\pi}} e^{\frac{-\theta^2}{2}} d\theta \geq \int_{-\emptyset_j(p_j)}^{\infty} \frac{1}{\sqrt{2\pi}} e^{\frac{-t^2}{2}} dt \tag{16}$$

where $\emptyset_j(p_j)$ is the value of the standard normal variation corresponding to the probability p_j.

$$-\frac{\overline{g_j}}{\sigma_{g_j}} \leq -\emptyset_j(p_j) \tag{17}$$

or

$$-\overline{g_j} + \sigma_{g_j}\emptyset_j \leq 0 \tag{18}$$

Eq. (17) can be rewritten as

$$\overline{g_j} - \sigma_{g_j}\emptyset_j \left[\sum_{i=1}^{N}\left(\frac{\partial g_j}{\partial y_i}\middle|\vec{\bar{Y}}\right)^2 {\sigma_{g_j}}^2\right]^{1/2} \geq 0 \tag{19}$$

Thus, the optimization problem of objective function f($\vec{Y}$) can be stated in its equivalent deterministic form.

2.4 Maximization of solar cell conversion efficiency

To maximize solar cell conversion efficiency, maximum absorption and minimum recombination are necessary for high conversion efficiency of a solar cell. The details of the computational procedure for finding the short-circuit current density, open-circuit voltage, and conversion efficiency are presented in the Appendix A.

The maximum operating power density (P_m) at one sun intensity can be found as

$$P_m = J_m V_m \tag{20}$$

For a sunlight concentration with intensity *C*, the equations for P_m, J_m and V_m can be obtained as

$$P_m(C) = J_m(C)V_m(C) \tag{21}$$

where $J_m(C)$ and $V_m(C)$ can be expressed by

$$J_m(C) = CJ_m \tag{22}$$

$$V_m(C) = V_m + V_T \log(C) \tag{23}$$

where the intensity of sunlight *C* can vary in the range of 1 to 100 suns and $V_T = \frac{KT}{nq}$ and the ideality factor (n), which is chosen to lie between 1 and 2 for simplicity, is a measure of how closely the diode follows the ideal diode equation. When a load is connected to the diode, a current will flow in the circuit

The following step-by-step procedure is used for the computation of conversion efficiency of a solar cell:

1. Calculate the total current density (J_L) using Eqs. (A-2) – (A-5)
2. Compute the reverse saturation current density (J_0) using Eqs. (A-6) – (A-10)
3. Compute the short-circuit current density (J_{SC}) derived from the results of the total current density (J_L) and the reverse saturation current density (J_0) using Eq. (A-11)
4. Compute the open-circuit voltage (V_{oc}) using Eq. (A-12)
5. Compute the maximum power density: $P_m = J_m V_m$ using Eq. (A-13)
6. Compute the maximum power density with the intensity of sunlight: $P_m(C) = J_m(C)\, V_m(C)$ using Eqs. (A-14)
7. Calculate total fractional power loss (F_{sum}) using Eqs. (A-15) – (A-28)

The following procedure is used to compute the power output developed by the cell:

1. – 5. Steps 1 through 5 are same as those indicated for the computation of the conversion efficiency
6. Multiply the maximum power density in step 5 by the area of solar cell ($W_c \cdot H_c$) to find the maximum power generated by the solar cell.

The objective is to find the optimal design vector $\vec{X}$ for maximization of the conversion efficiency to reduce power losses under concentrated sunlight (C), and can be stated as a maximization problem as

$$\text{Maximize f } (\vec{X}) = \frac{J(C)_m V(C)_m}{P_{in} \cdot C}(1 - F_{sum}) \times 100 \tag{24}$$

Solar cell conversion efficiency is related to short-circuit current (J_{sc}), open-circuit voltage (V_{oc}), incident power density (P_{in}) at 1 sun, concentrated sunlight (C) and fractional power losses (F_{sum}). The power losses (F_{sum}) from metallic contacts largely consist of the surface sheet (F_{sr}), contact (F_c), grid metal of fingers (F_f), bus bars resistivity (F_b) and shadowing (F_s). The total fractional power loss (F_{sum}) can be expressed in terms of the individual fractional power loss as

$$F_{sum} = F_{sr} + F_f + F_b + F_s + F_c \tag{25}$$

The design of the top contact considers geometric parameters of metal grids to minimize their resistance in addition to the overall reduction of power losses associated with the geometric grid contact factors. The main concerns of geometric grid contact factors are the finger and busbar spacing, the metal height-to-width aspect ratio, the minimum metal grid of width and height, and the resistivity of the metal. Accordingly, the design variables of the problem, for a rectangular solar cell, can be laid out as

$$\vec{X}=\begin{Bmatrix} T_e \\ T_b \\ W_c \\ H_c \\ W_f \\ H_f \\ N_f \\ W_b \\ H_b \\ N_b \\ C \end{Bmatrix} \equiv \begin{Bmatrix} x_1 \\ x_2 \\ x_3 \\ x_4 \\ x_5 \\ x_6 \\ x_7 \\ x_8 \\ x_9 \\ x_{10} \\ x_{11} \end{Bmatrix} \quad (26)$$

The random variable vectors are:

$$\vec{Y}=\begin{Bmatrix} T_e \\ T_b \\ W_c \\ H_c \\ W_f \\ H_f \\ W_b \\ H_b \\ P_{in} \\ \rho_m \\ R_c \\ R_{sh} \end{Bmatrix} \equiv \begin{Bmatrix} y_1 \\ y_2 \\ y_3 \\ y_4 \\ y_5 \\ y_6 \\ y_7 \\ y_8 \\ y_9 \\ y_{10} \\ y_{11} \\ y_{12} \end{Bmatrix} \quad (27)$$

Geometric design variables except for integer values, such as the number of fingers (N_f), busbars (N_b), and concentrated sunlight (C) are considered random variables because these design factors are dependent on the manufacturing production conditions related to tolerances. The incident power density (P_{in}) varies in a particular location due to atmospheric effects. Furthermore, the metal property (ρ_m) of the fingers and busbars, the contact resistance (R_c), and the resistance of the sheet (R_{sh}) depend on the purity of materials and fabrication skills.

The optimization problem is solved by placing lower and upper bounds on the design variables as $x_i^{(l)} \leq x_i \leq x_i^{(u)}$; $i = 1\ to\ 11$, with the bounds indicated in Table 1:

Table 1 Lower and upper bounds on the design variables

i	1	2	3	4	5	6	7	8	9	10	11
$x_i^{(l)}$	0.1μm	100μm	0.5cm	0.5cm	20μm	4.6μm	2	100μm	4.6μm	2	1
$x_i^{(u)}$	8μm	450μm	5cm	5cm	200μm	50μm	100	4000μm	50μm	10	100

The constraints of the optimization problem can include relationships between the height of the finger (H_f) and the busbar (H_b) by considering the delivery to the busbars and the shading from the busbars, the ratio of width to height of the finger, and the spacing (D) between the fingers and the busbars.

$$D_f - \left(W_c - W_f \cdot N_f\right)/\left(N_f - 1\right) = 0 \tag{28}$$

$$W_f \cdot N_f - W_c \leq 0 \tag{29}$$

$$D_b - (H_c - W_b \cdot N_b)/(N_b - 1) = 0 \tag{30}$$

$$W_b \cdot N_b - H_c \leq 0 \tag{31}$$

$$0 \leq H_f - H_b \leq 1\mu\text{m} \tag{32}$$

$$0.23 \leq \frac{H_f}{W_f} \leq 0.25 \tag{33}$$

The MATLAB program can implement the optimization of solar PV collector system performance based on Genetic Algorithms (GA) method by using the function of *ga*, which finds mixed-integer values of the minimum of a scalar function of several variables, starting with an initial value of design parameters.

2.5 Probabilistic optimization

The new objective of the probabilistic optimization problem (F) is constructed by the combination of the mean value of the objective function ($\bar{f}$) and standard deviation of a solar cell (σ_f) with the weight values of k_1 and k_2 . By virtue of this, a new objective function (F) based on a set of random variables can be expressed as

$$\mathrm{f(Y)} = k_1\bar{f} + k_2\sigma_f \tag{34}$$

The weighted mean $k_1\bar{f}$ and the weighted variation $k_2\sigma_f$ can be expressed as

$$k_1\bar{f} \approx k_2\sigma_f \tag{35}$$

and then rewritten as

$$k_2 \approx \frac{k_1\bar{f}}{\sigma_f} \tag{36}$$

If the weight of the mean k_1 is equal to 1, the value of the weight of variation k_2 is decided by Eq. (36), and the value of the weight of variation, k_2, depends on the mean values of random variables and their coefficient of variations.

The deterministic optimization method is used to predict optimal cell (design) and a solar cell design without considering the stochastic behaviors. Therefore, the stochastic approach presents more as complex and involves statistical processing for reliability.

2.6 Illustrative example and numerical results

The MATLAB program can implement the optimization of a solar cell performance based on the genetic algorithms (GA) method by using the function of *ga*, which finds mixed-integer values of the minimum of a scalar function of several variables, starting with an initial value of the design parameters.

The values of the coefficient are applied from 0.02 to 0.1 because there is no feasibility after the coefficient of variation exceeds 0.1. Table 2 and Fig. 1 show the values of k_2 and the variations of conversion efficiency in a square and a rectangular cell with a coefficient variation under the probability of a constraint satisfaction of 60 %. The conversion efficiencies (η_c) are steeply decreased from 20.284 % to 20.262 % at a coefficient of variation of 0.06 for a square cell and from 20.541 % to 20.525 % at a coefficient of variation of 0.08 for a rectangular cell. A detailed discussion of the influences with various probabilities of constraint satisfaction and coefficient of variations is conducted in this section.

Table 2 Values of k_2 and the coefficient variations

Coefficient variation		0.02	0.04	0.06	0.08	0.1
k_2	Square	448	223	149	111	88
	Rectangular	582	291	193	143	115

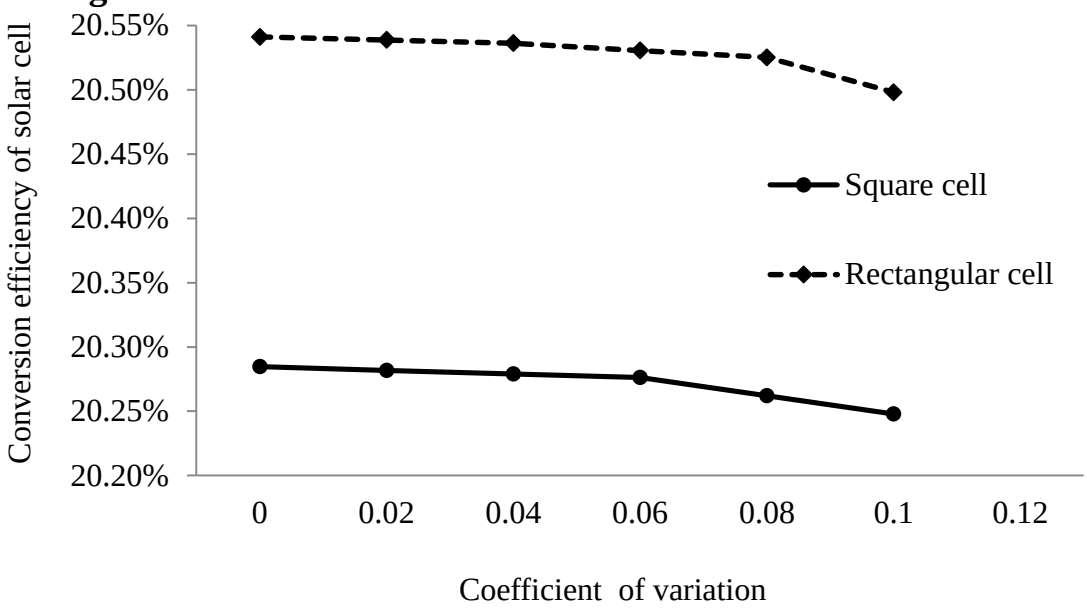

Fig. 1 Comparison of conversion efficiency between square and rectangular cells under coefficient of variation

The influence of probability of constraint satisfaction and coefficient variation of random variables is observed. The new objective function, F, is maximized with different values of the probability of constraint satisfaction. The values of probability of constraint satisfaction are 50 %, 80 %, 90 %, 95 %, 99 %, and 99.997 % with 0.5 %, 1.0 %, 1.5 %, and 2.0 % of coefficients of variation, respectively. Variations of mean conversion efficiency, $\bar{f}$, standard deviations, σ_f, and new objective function, F, are investigated through the design variables with respect to the probability of constraint satisfaction.

All design variables start to shift under different probabilities of constraint satisfaction and coefficients of variation. Figure 2 shows variations of design variables under varying values of coefficients of variation and probability of constraint satisfaction.

❖ 0.005 of coefficient of variation

- Square cell

The conversion efficiency is decreased from 20.284 % to 20.260 % as shown in Table 2 under a probability of constraint satisfaction between 50 % and 99.997 %. The value of standard deviation is decreased from 1.129E – 04 to 1.106E – 04. Individual design variables are examined below in further detail.

As shown in Figs. 2 (a) - (b), the thicknesses of the emitter and base are associated with a decrease in conversion efficiency; meanwhile, the probabilities of constraint satisfaction and variations of coefficient are increased. The thickness of the emitter is in a range between 7.56 μm and 7.78 μm, but the thickness of the base is dramatically decreased from 415 μm to 254 μm under a probability of constraint satisfaction between 50 % and 99.997 %, respectively.

The cell length (L_c) is increased from 0.80 cm up to 0.84 cm. The width of the fingers, as shown in Figs. 2 (d) and (e), is augmented from 20 μm to 20.43 μm at 99.997 % of probability of constraint satisfaction. Also, the width of the busbars is increased from 100 μm to 102.40 μm at 99.997 % of probability of constraint satisfaction. The heights of the fingers and busbars, as shown in Figs. 2 (f) and (g), are increased from 50 % to 99 % of probability of constraint satisfaction. However, after the probability exceeds 99 % of probability of constraint satisfaction, H_f is steeply increased from 4.91 μm to 4.97 μm . However, H_b is decreased from 6.01 μm to 5.82 μm because the number of busbars is modified. In selecting the number of fingers, the amount is reduced from 18 to 17, yet the number of busbars is constant at 2 as shown in Figs. 2 (h) and (i). The optimum value of intensity of sunlight is 6, though the larger cells begin to diminish in size as the intensity of sunlight reaches 5 at 99.997 % of probability of constraint satisfaction. This

grants larger solar cells greater influence on the reduction of intensity of sunlight for conversion efficiency (η_c) as shown in Figs. 2 (j).

- Rectangular cell

The conversion efficiency is decreased from 20.541 % to 20.524 % as shown in Table 2 under a probability of constraint satisfaction between 50 % and 99.997 %. The value of standard deviation is increased from 8.807E – 05 to 8.947E – 04. A detailed discussion of the role of each design variable will follow.

As shown in Figs. 2 (a) - (b), the thickness of the emitter is in a range between 7.99 µm and 7.96 µm, but the thickness of the base is increased considerably from 252 µm to 406 µm under a probability of constraint satisfaction between 50 % and 99.997 %, respectively. The cell length (L_c) is increased from 1.76 cm up to 2.44 cm; the length of height (H_c) is almost constant at 0.50 cm. Figures 2 (d) and (e) demonstrate a clear increase in the width of the fingers from 20.09 µm to 20.26 µm at 99.997 % of probability of constraint satisfaction. The width of the busbars is similarly increased from 100 µm to 101.31 µm at 99.997 % of probability of constraint satisfaction. As shown in Figs. 2 (f) and (g), the height of the fingers (H_f) is decreased from 5.00 µm to 4.92 µm under a probability of constraint satisfaction between 50 % and 99.997 %. The height of the busbars (H_b) is decreased from 6.01 µm to 5.82 µm as shown in Figs. 2 (h) and (i). In the case of the fingers, the number of fingers is the same at 12, but the number of busars is increased from 2 to 3 as shown in Figs. 2 (h) and (i). The optimum value of intensity of sunlight is 6 as shown in Figs. 2 (j).

Table 2 Mean values and standard deviations of objective of probability optimization under different constraint satisfaction and 0.005 of coefficient of variation

Coefficient variation Of standard deviation		Probability of constraint satisfaction	$\bar{f}$	F	σ_f
			Optimal	Optimal	Optimal
0.005	Square	50%	0.20284	0.40568	1.129E-04
	Rectangular		0.20541	0.41823	8.807E-05
	Square	80%	0.20282	0.40563	1.130E-04
	Rectangular		0.20539	0.41078	8.811E-05
	Square	90%	0.20281	0.40560	1.129E-04
	Rectangular		0.20538	0.41076	8.816E-05
	Square	95%	0.20280	0.40560	1.133E-04
	Rectangular		0.20537	0.41074	8.823E-05
	Square	99%	0.20277	0.40554	1.129E-04
	Rectangular		0.20534	0.41069	8.855E-05
	Square	99.997%	0.20260	0.40520	1.106E-04
	Rectangular		0.20524	0.41049	8.947E-04

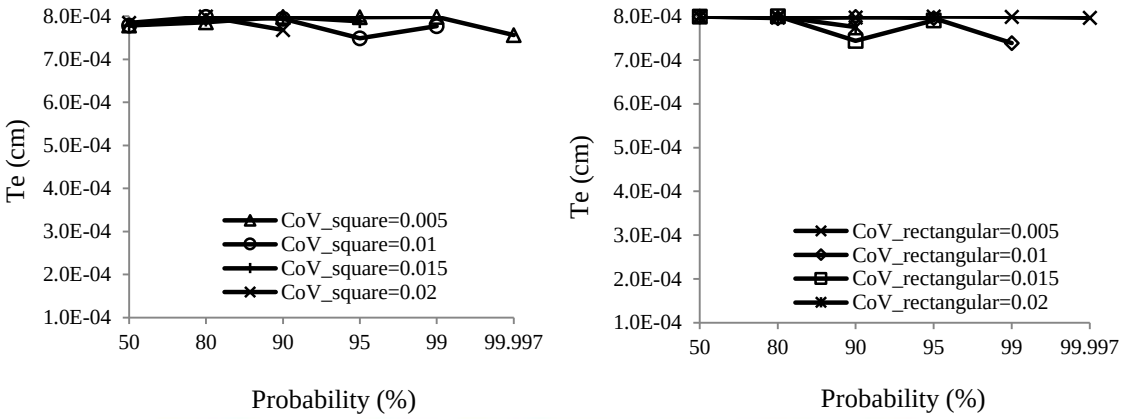

(a)

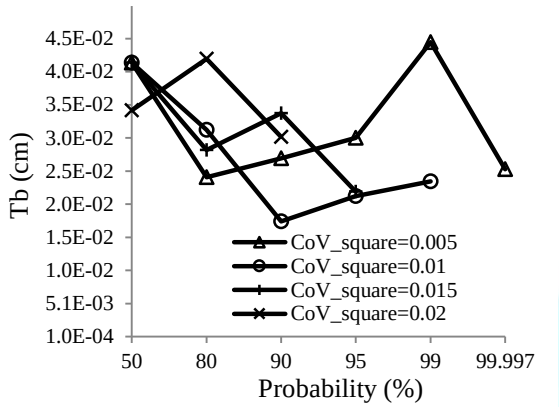
4.5E-02
4.0E-02
3.5E-02
3.0E-02
2.5E-02
2.0E-02
1.5E-02
1.0E-02
5.1E-03
1.0E-04
Tb (cm)
50
80
90
95
99
99.997
Probability (%)
CoV_square=0.005
CoV_square=0.01
CoV_square=0.015
CoV_square=0.02

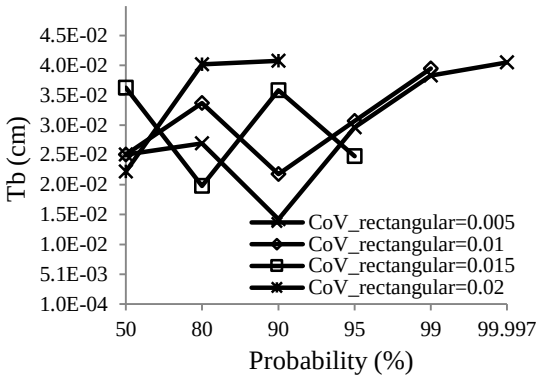
4.5E-02
4.0E-02
3.5E-02
3.0E-02
2.5E-02
2.0E-02
1.5E-02
1.0E-02
5.1E-03
1.0E-04
Tb (cm)
50
80
90
95
99
99.997
Probability (%)
CoV_rectangular=0.005
CoV_rectangular=0.01
CoV_rectangular=0.015
CoV_rectangular=0.02

(b)

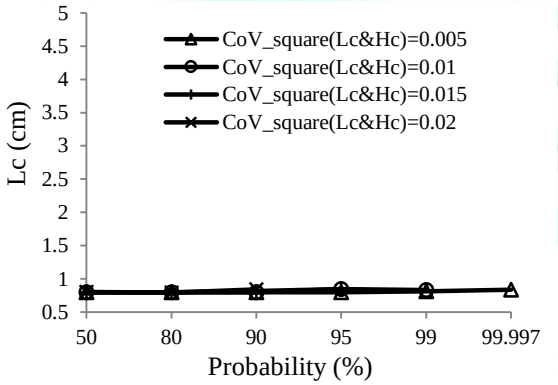
5
4.5
4
3.5
3
2.5
2
1.5
1
0.5
Lc (cm)
50
80
90
95
99
99.997
Probability (%)
CoV_square(Lc&Hc)=0.005
CoV_square(Lc&Hc)=0.01
CoV_square(Lc&Hc)=0.015
CoV_square(Lc&Hc)=0.02

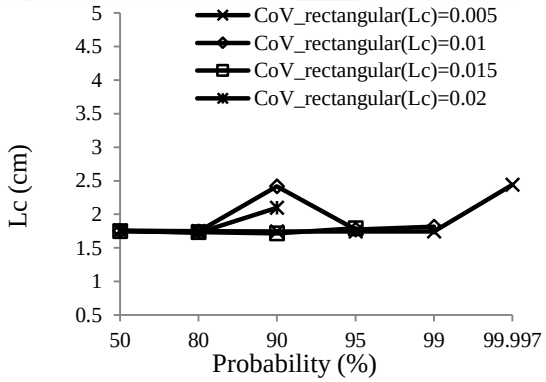
5
4.5
4
3.5
3
2.5
2
1.5
1
0.5
Lc (cm)
50
80
90
95
99
99.997
Probability (%)
CoV_rectangular(Lc)=0.005
CoV_rectangular(Lc)=0.01
CoV_rectangular(Lc)=0.015
CoV_rectangular(Lc)=0.02

(c) - 1

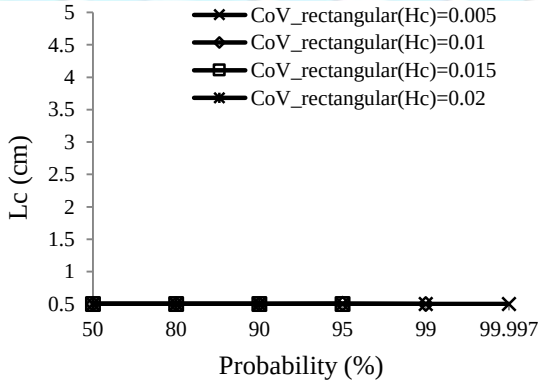
5
4.5
4
3.5
3
2.5
2
1.5
1
0.5
Lc (cm)
50
80
90
95
99
99.997
Probability (%)
CoV_rectangular(Hc)=0.005
CoV_rectangular(Hc)=0.01
CoV_rectangular(Hc)=0.015
CoV_rectangular(Hc)=0.02

(c) - 2

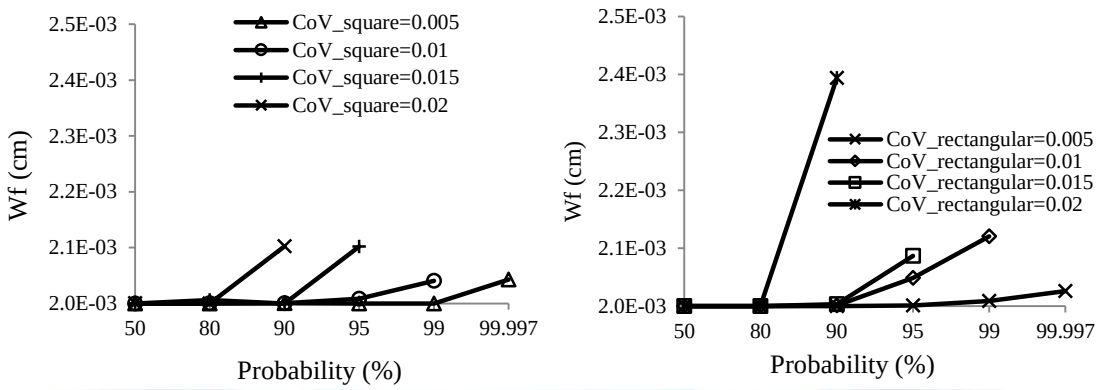
2.5E-03
2.4E-03
2.3E-03
2.2E-03
2.1E-03
2.0E-03
Wf (cm)
CoV_square=0.005
CoV_square=0.01
CoV_square=0.015
CoV_square=0.02
50
80
90
95
99
99.997
Probability (%)
CoV_rectangular=0.005
CoV_rectangular=0.01
CoV_rectangular=0.015
CoV_rectangular=0.02

(d)

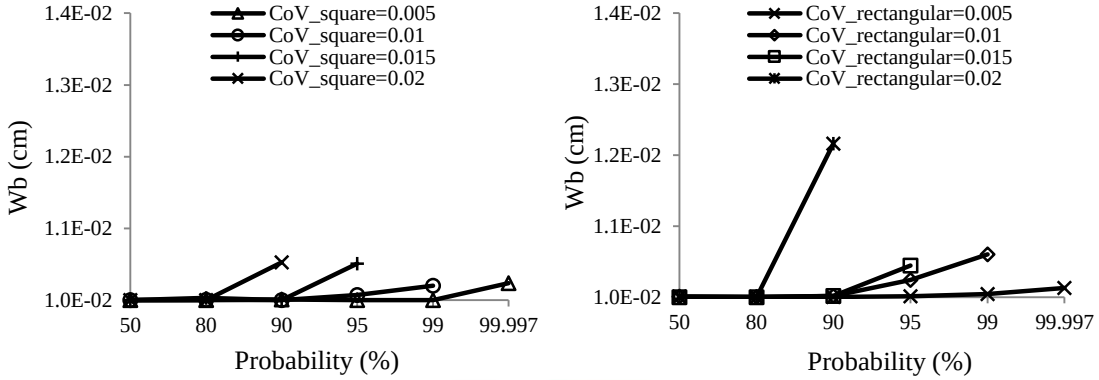
1.4E-02
1.3E-02
1.2E-02
1.1E-02
1.0E-02
Wb (cm)
CoV_square=0.005
CoV_square=0.01
CoV_square=0.015
CoV_square=0.02
50
80
90
95
99
99.997
Probability (%)
CoV_rectangular=0.005
CoV_rectangular=0.01
CoV_rectangular=0.015
CoV_rectangular=0.02

(e)

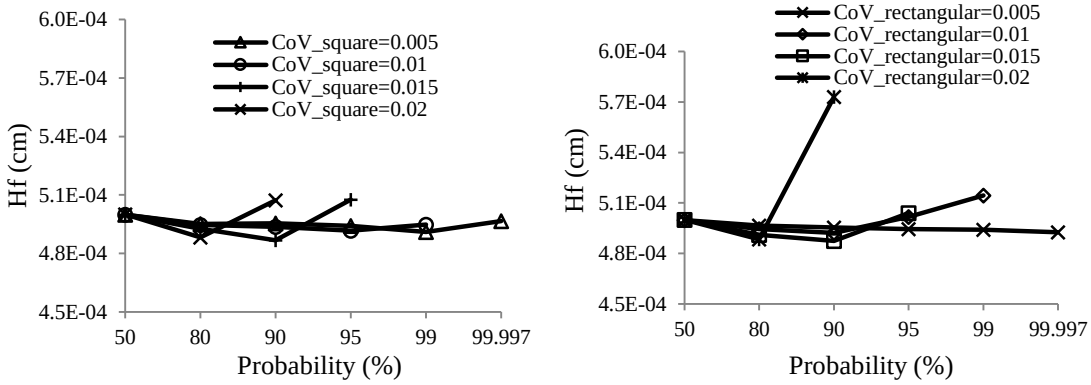
6.0E-04
5.7E-04
5.4E-04
5.1E-04
4.8E-04
4.5E-04
Hf (cm)
CoV_square=0.005
CoV_square=0.01
CoV_square=0.015
CoV_square=0.02
50
80
90
95
99
99.997
Probability (%)
CoV_rectangular=0.005
CoV_rectangular=0.01
CoV_rectangular=0.015
CoV_rectangular=0.02

(f)

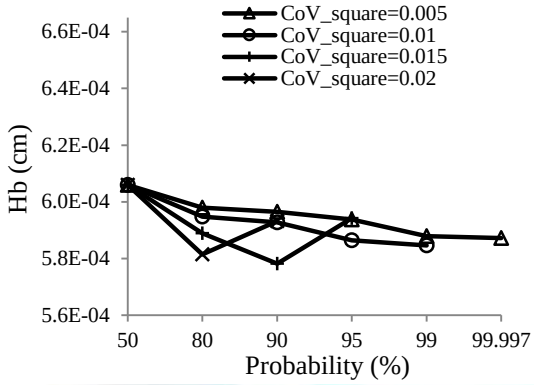
CoV_square=0.005
CoV_square=0.01
CoV_square=0.015
CoV_square=0.02
Hb (cm)
6.6E-04
6.4E-04
6.2E-04
6.0E-04
5.8E-04
5.6E-04
50
80
90
95
99
99.997
Probability (%)

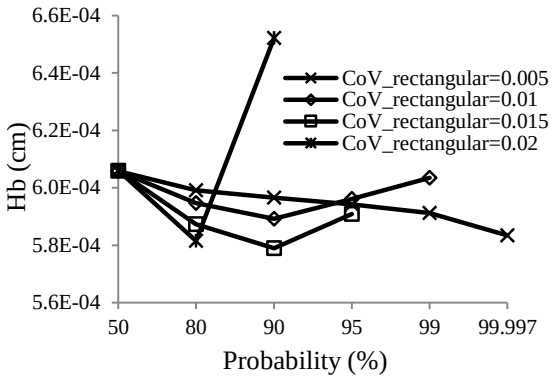
CoV_rectangular=0.005
CoV_rectangular=0.01
CoV_rectangular=0.015
CoV_rectangular=0.02
Hb (cm)
6.6E-04
6.4E-04
6.2E-04
6.0E-04
5.8E-04
5.6E-04
50
80
90
95
99
99.997
Probability (%)

(g)

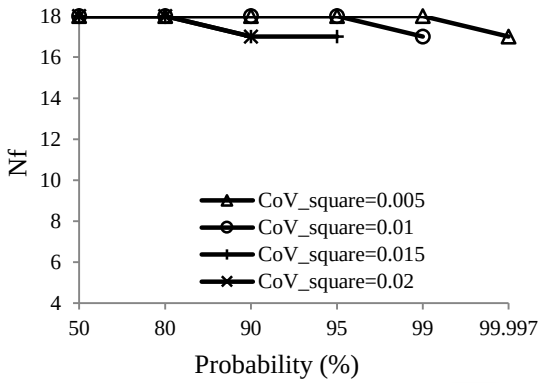
CoV_square=0.005
CoV_square=0.01
CoV_square=0.015
CoV_square=0.02
Nf
18
16
14
12
10
8
6
4
50
80
90
95
99
99.997
Probability (%)

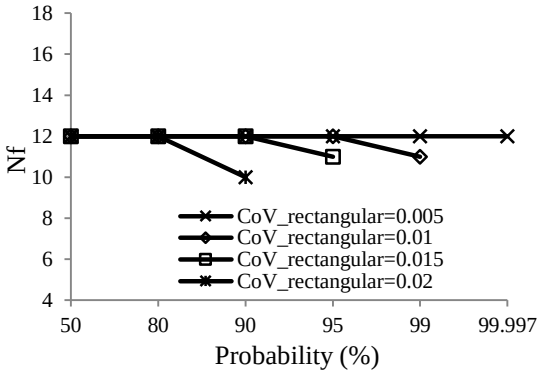
CoV_rectangular=0.005
CoV_rectangular=0.01
CoV_rectangular=0.015
CoV_rectangular=0.02
Nf
18
16
14
12
10
8
6
4
50
80
90
95
99
99.997
Probability (%)

(h)

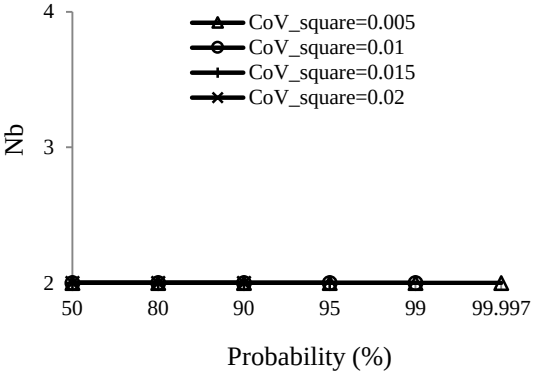
CoV_square=0.005
CoV_square=0.01
CoV_square=0.015
CoV_square=0.02
Nb
4
3
2
50
80
90
95
99
99.997
Probability (%)

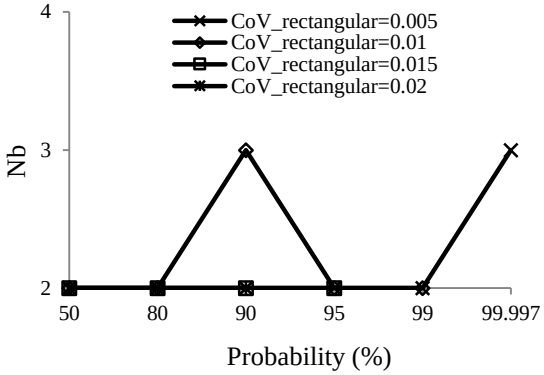
CoV_rectangular=0.005
CoV_rectangular=0.01
CoV_rectangular=0.015
CoV_rectangular=0.02
Nb
4
3
2
50
80
90
95
99
99.997
Probability (%)

(i)

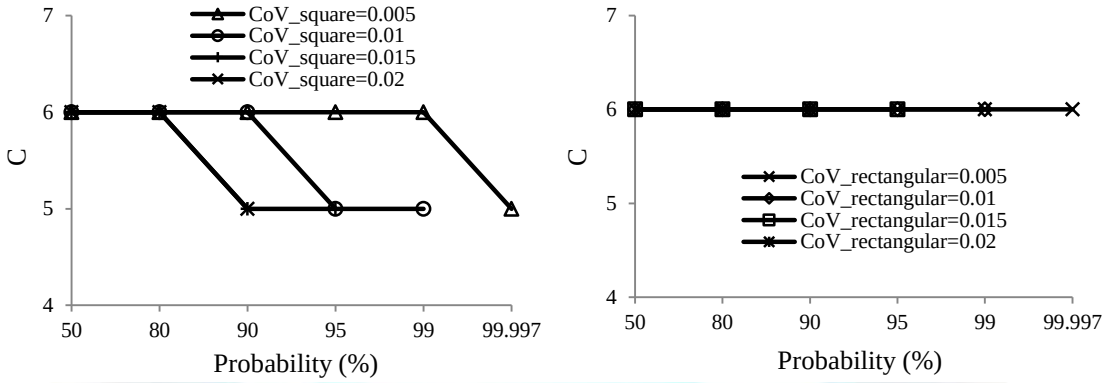

(j)

Fig. 2 Results of design variables under coefficient variation and probability of constraint satisfaction

3. Fuzzy set analysis

3.1 Fuzzy set analysis

The conversion efficiency is obtained by using the function of *ga* MATLAB program. The maximum conversion efficiencies (η_{ma}) are 20.28 % and 20.54 %, respectively. The conversion efficiency in the fuzzy membership function is associated with geometric design parameters including the surface sheet, contact between the solar cell and grid metal contact, grid metal of fingers, busbars, and the shadowing from grid metal parts except for integer design values of a number of fingers and busbars, and intensity of sunlight. Thus, the uncertain input parameters, similarly, consist of 7 and 8 design parameters and all 4 uncertain design parameters in a square cell and a rectangular cell, respectively. As a result, the uncertain input parameters of the solar cell are applied to the fuzzy set analysis in the same way as uncertain input parameters.

The uncertain input parameters are

$$\vec{Y}=\begin{Bmatrix} P_{in} \\ \rho_m \\ R_c \\ R_{sh} \\ T_e \\ T_b \\ L_c \\ H_c \\ W_f \\ H_f \\ W_b \\ H_b \end{Bmatrix} \equiv \begin{Bmatrix} Y_1 \\ Y_2 \\ Y_3 \\ Y_4 \\ Y_5 \\ Y_6 \\ Y_7 \\ Y_8 \\ Y_9 \\ Y_{10} \\ Y_{11} \\ Y_{12} \end{Bmatrix} \quad (37)$$

±1 %, ±2 %, ±3 %, ±4 % and ±5 % of the fuzzy confidence intervals are applied to solar cell for observing the deviations varying the α-cut interval levels from crisp value.

3.2 Numerical results

In the case of a square cell, ±1 %, ±2 %, ±3 %, ±4 % and ±5 % of the fuzzy confidence interval, the percent deviations of solar cell conversion efficiency show the results of responses of 5.61 % and 25.15 % in the lower bound section and 5.90 % and 20.97 % to applying uncertain input parameters. Figures 3 (a) and (b) show the deviations from the crisp value in conversion efficiency and Figs. 4 (a) and (b) show the variations of the triangular shapes of a square cell and a rectangular cell. Conversion efficiency is associated with power losses, and the response to applying uncertain input parameters to a solar cell are observed with the example of ±2 % of fuzzy confidence interval in a square cell and a rectangular cell, respectively.

The crisp value of the total fractional power loss (F_{sum}) is 11.08 % at 20.28 % of the conversion efficiency. The total power loss (F_{sum}) becomes 2.38 % of the total power loss in the lower bound and 19.18 % of the total power loss in the upper bound. The total power loss reduced by the main individual fractional power loss is from the shadowing loss. The shadowing loss is 1.49 % in the lower bound and 14.64 % in the upper bound. These results indicate that the shadowing loss is caused by the size and number of fingers and busbars blocking sunlight.

In the case of ±2 % uncertain fuzzy confidence interval of the rectangular cell, the crisp value of the total fractional power loss (F_{sum}) is 9.93 % at 20.54 % of conversion efficiency. The total power loss becomes 1.39 % in the lower bound and 17.86 % in the upper bound. The main fractional power loss in the total power loss is from shadowing loss. The shadowing loss is 0.5 % in the lower bound and 13.69 % in the upper bound. Also, these results indicate that the shadowing loss is increased alongside any increases in the cell size and number of fingers and busbars, which contribute to the blockage of sunlight.

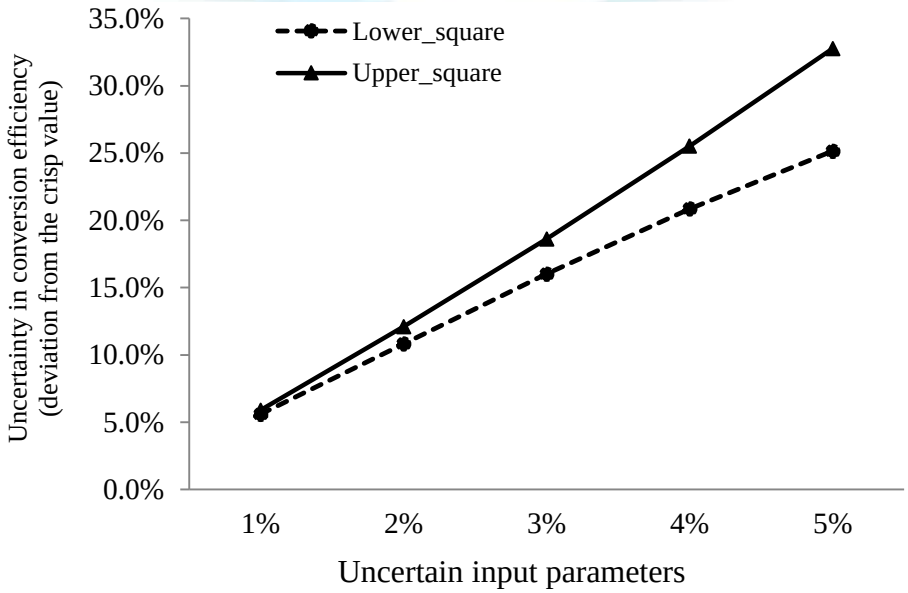

(a) Uncertainty in conversion efficiency of a square cell

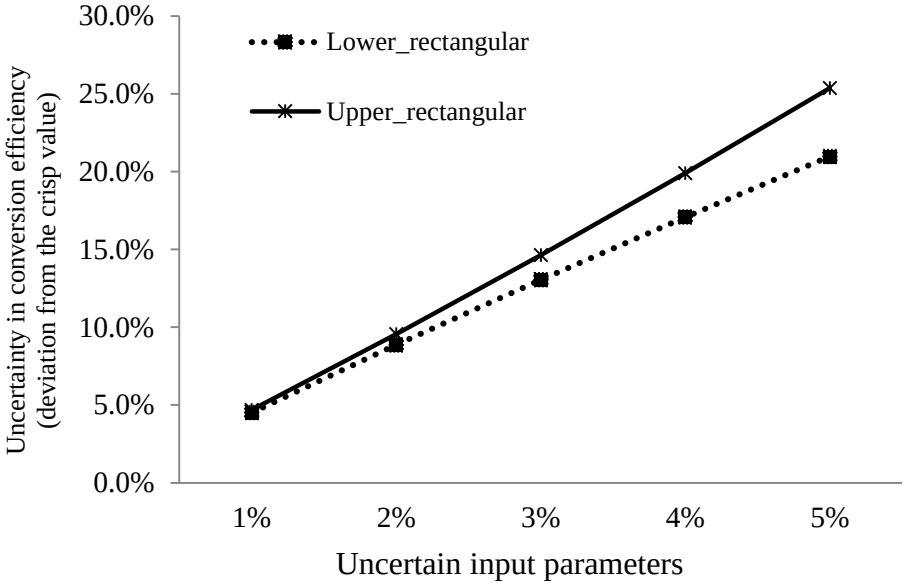

(b) Uncertainty in conversion efficiency of a rectangular cell

Fig. 3 Variation of deviations from the crisp value in conversion efficiency

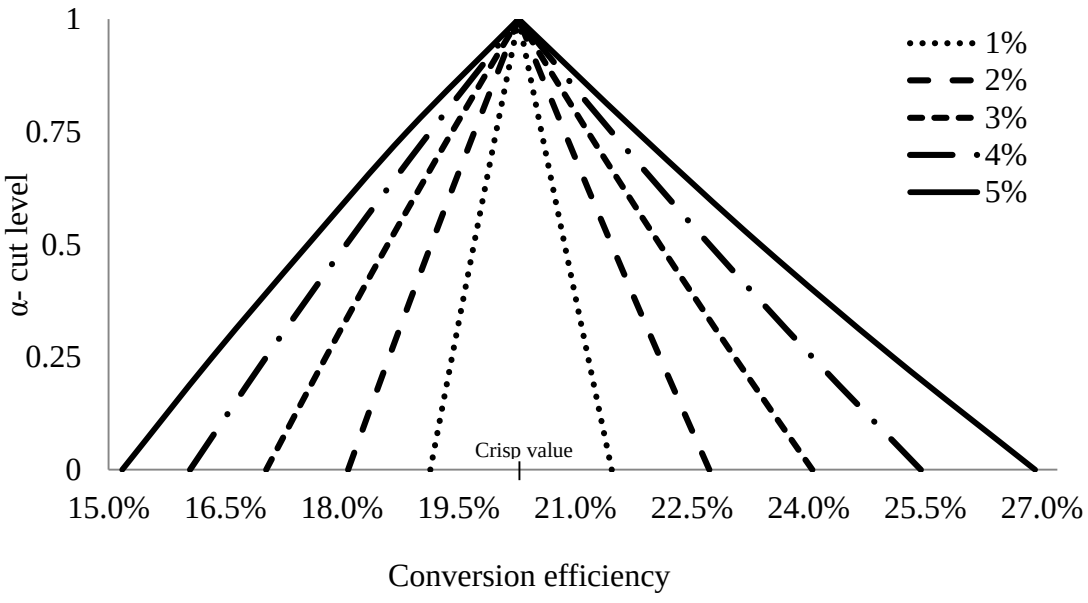

(a) Conversion efficiency of square cell

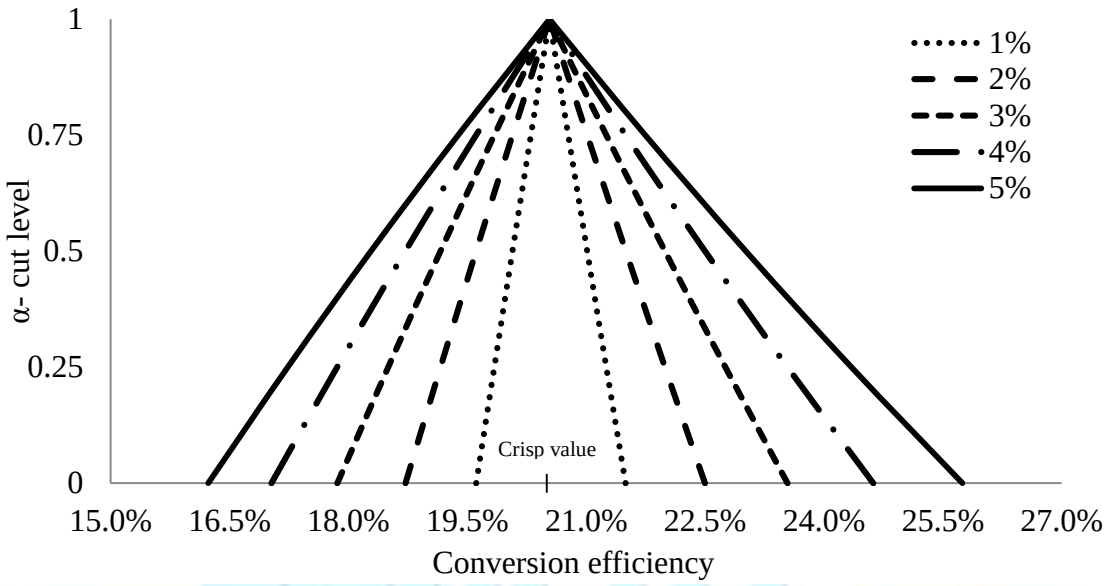

(b) Conversion efficiency of rectangular cell

Fig. 4 Variation of triangular shapes from the crisp value in conversion efficiency with respect to a fuzzy confidence interval

In the case of the conversion efficiency, Y_1, and Y_7 of uncertain input parameters mainly influence the deviation of the conversion efficiency. Y_1 is constant solar energy and Y_7 is the length of a solar cell in a square cell as shown in Fig. 5 (a). Similarly, Y_1, Y_7, and Y_8 are constant solar energy, and the length of a solar cell as shown in Fig. 5 (b).

In the case of the square cell, except for Y_1 and Y_8, other uncertain parameters contribute to the deviation at less than 1 %. Y_1 of an uncertain parameter is associated with the conversion efficiency ($\eta = \frac{J(C)_m V(C)_m}{P_{in}\ C}$ (1- F_{sum})). Thus, at ±5 % of the fuzzy confidence interval, 4.76 % and 5.26 % of deviations in both bounds are similar variations of uncertain input parameters, respectively. Y_7 of an uncertain input parameter is the main factor influencing the deviation of the conversion efficiency because the Y_7 parameter is associated with the fingers and busbars. The lengths of cells (W_c and H_c) are related to the length of the fingers and busbars in both a square cell and a rectangular cell. Similarly, in the case of the rectangular cell, at ±5 % of the fuzzy confidence interval, Y_1 is related to the conversion efficiency. Thus, the deviations of 4.76 % and 5.26 % are estimated. Y_7 and Y_8 of uncertain parameters are associated with the fingers and busbars, which are related to the contact power loss (F_c) between metallic fingers and busbars and solar cell surface and shadowing loss. When the lengths of the square and the rectangular cells increase from ±1 % to ±5 %,

respectively, the deviation values become larger than the applied value of interval range. These results indicate that the fingers and busbars are related to the power losses of contact resistance (F_c), metal resistivity (F_f and F_b) and shadowing (F_s). When a single uncertain parameter is not incorporated with other uncertain input parameters, there is a small deviation, but with related factors between the length of the cells and the fingers or busbars, they significantly affect the deviation of the conversion efficiency.

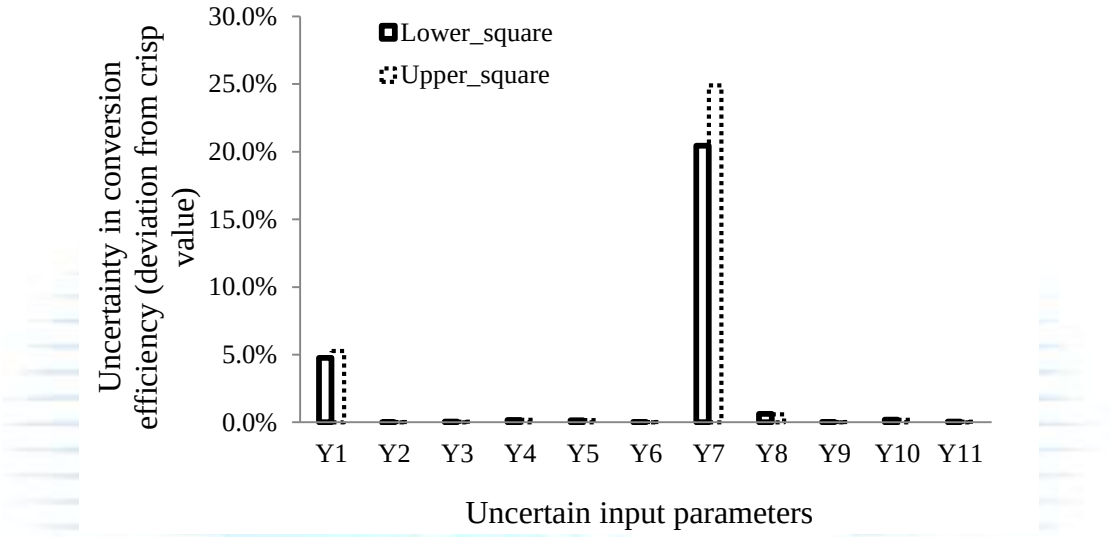

(a) Influence on conversion efficiency of square cell with respect to uncertain input parameters

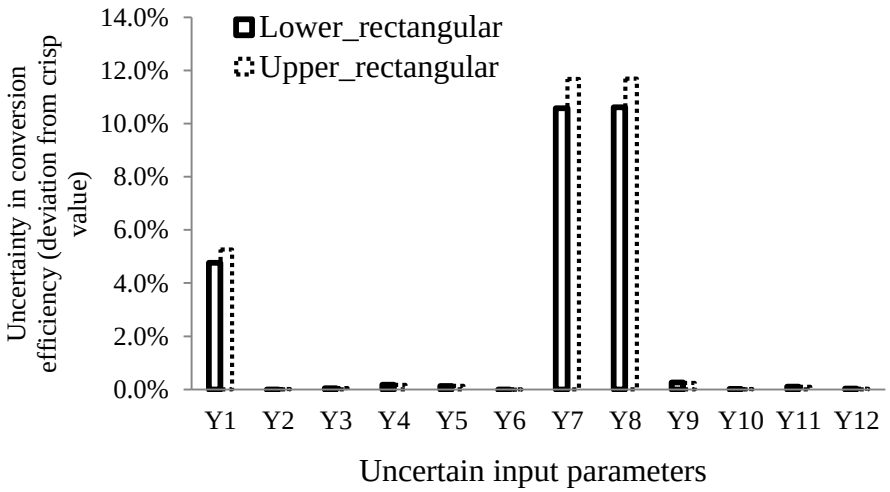

(a) Influence on conversion efficiency of rectangular cell with respect to uncertain input parameters

Fig. 5 Influence on conversion efficiency with respect to uncertain input parameters

4. Conclusions

Probabilistic optimization and fuzzy set analysis techniques used in a solar cell have been estimated. The results of probabilistic optimization are obtained by varying the values of the weight of mean and coefficients of variation, and the results of fuzzy set analysis are gained by applying values of α-cut level and fuzzy confidence interval. This work illustrates the parametric study involved in the probabilistic performance of a solar cell.

When the probability of constraint satisfaction is 50 %, all design variables have nearly the same results as the coefficient variations of the random factors because the probabilistic method retrogresses to deterministic optimization at different levels of uncertainty of the random variables. As the values of probability of constraint satisfaction increase from 50%, the constraints become more rigid, suggesting an optimization problem is solved by enforcing limited constraints compared to deterministic optimization conditions. The length of a cell, the height of the fingers and busbars, and the number of fingers are changed by applying different values of probability of constraint satisfaction and coefficient of variation in both cells. The change in geometric design variables has an influence on behavior constraints regarding the relationship between the height of the fingers and busbars, the aspect ratio of width to height of the fingers and busbars, and the numbers of fingers and busbars. As a result, most of the design variables start to vary considerably with varying coefficients of variation and probabilities of constraint satisfaction in both cells for observing the influence of uncertainty on the performance. In application, the change of probability of constraint satisfaction and coefficient of variation should be considered for solar cell design and manufacturing because randomness can lead to performance deviations in finding optimized solutions and obtaining effective performance uniformly across many data sets.

The deviations of solar cell performance of the conversion efficiency are investigated. The design of a solar cell should be considered with top contact design. The conversion efficiency is associated with cell size and the geometric parameters of the fingers and busbars. As observed from the present results, the main considerations of optimal cell design are the cell size and metallic parts (fingers and busbars) because the total power loss is dominated by the contact loss between metallic parts and the size and number of fingers and busbars, which mainly cause shadowing loss.

[References]

[1] Arturo, M.A, 1985, Optimum concentration factor for silicon solar cells, *Solar Cells*, Vol. 14, pp. 43-49.

[2] Rault, F.K., 2002, A probabilistic approach to determine radiative recombination carrier lifetimes in quantum well solar cells, *Microelectronics Journal*, Vol. 34, pp. 265-270

[3] Hengsritawat, V., 2012, Optimal sizing of photovoltaic distributed generators in a distribution system with consideration of solar radiation and harmonic distortion, *Electrical Power and Energy Systems*, Vol. 39, pp.36-47

[4] Zulkifli, N.A., 2014, Probabilistic Analysis of Solar Photovoltaic Output Based on Historical Data, *IEEE 8th International Power Engineering and Optimization Conference*, pp. 133-137

[5] Zadeh, L., 1965, Fuzzy sets, Inform, Control 8, pp.338-353

[6] Bellman, R.E., Zadeh, L.A., 1970, Decision making in a fuzzy environment, *Management Science*, 17, pp.141-164

[7] Emam, O.E., 2006, A fuzzy approach for bi-level integer non-linear programming problem, *Applied Mathematics and computation*, 172, pp.62-71

[8] Liang, T.F., 2008, Fuzzy multi-objective production/distribution planning decisions with multi-product and multi-time period in a supply chain, *Computers & Industrial Engineering*, 55, pp.676-694

[9] Jain, S.C, Heasell, E.L and Roulston, D.J., 1987, Recent advances in the physics of silicon P-N junction solar cells including their transient response, *Prog. Quant. Electr*., Vol.11, No. 2, pp. 105-204.

[10] Singal, C.M, 1981, Optimum cell size for concentrated-sunlight silicon solar cells, *Solar Cells*, Vol. 3, No. 1, pp. 9-16.

[11] Liu, W., Li, Y., Chen, J., Chen, Y., Wang, X., and Yang, F., 2010, Optimization of grid design for solar cells, *Journal of Semiconductors*, Vol.31, No. 1, pp. 0140061-4.

[12] Shabana, M. M., Saleh M.B., Soliman M.M., 1988, Optimization of grid design for solar cells at different illumination levels, *Solar cells*, Vol. 26, No. 3, pp.177-187

Nomenclature

C = Intensity of sunlight (an integer)

D_b= Spacing between the busbars (cm)

D_f = Spacing between the fingers (cm)

D_p = Minority electron diffusion coefficient (cm^2/s)

D_n = Minority hole diffusion coefficient (cm^2/s)

F_b =Fractional power loss of the resistivity of the busbars (%)

F_c = Fractional power loss of contact resistance (%)

F_f = Fractional power loss of the resistivity of the fingers (%)

F_{sum} = Total fractional power losses (%)

F_s = Fractional power loss of shadowing (%)

F_{sr} = Fractional power loss of sheet resistance (%)

H_c = Height of cell (cm)

J_B = Current density of base (mA/cm^2)

J_E = Current density of emitter (mA/cm^2)

J_L= Light-generated current density (mA/cm^2)

J_m = Maximum operating current density (mA/cm^2)

J_{SCR} = Current density of space-charge region (mA/cm^2)

J_S = Saturation current density (mA/cm^2)

J_{sc} = Short-circuit density (mA/cm^2)

k = Boltzmann constant (8.617×10^{-5} eV/K)

L_p = Minority electron diffusion length (μm)

L_n = Minority hole diffusion length (μm)

L_T = Current transfer length (μm)

L_c = Length of cell (cm)

N_a = Acceptor concentration (cm^3)

N_d = Donor concentration (cm^3)

n_i = Intrinsic carrier concentration (cm^3)

n_{ph} = Photon flux ($cm^{-2}\ s^{-1}$)

P_m = Maximum operating power density (W/cm^2)

P_{in} = Input incident power density (W/m^2)

P_o = Power output (W)

q = Electron charge ($1.602\times10^{-19}\ colulomb$)

R = Reflection coefficient of the anti-reflective coating

R_{sh} =Sheet resistance (Ω/cm^2)

S_p = Recombination velocity of the front surface (cm/s)

S_n = Recombination velocity of the back surface (cm/s)

t_{scr} = Width of the space charge region (μm)

T = Temperature (K)

T_e = Thickness of the emitter region (μm)

T_b = Thickness of the base region (μm)

V_{oc} = Open-circuit voltage (mV)

V_m = Maximum operating voltage (mV)

W_c = Width of cell (cm)

α = Absorption coefficient (cm^{-1})

η_c = Conversion efficiency of a solar cell (%)

η_{max_c} = Maximum conversion efficiency of a solar cell (%)

τ_p = Minority carrier lifetime in the emitter region (μs)

τ_n= Minority carrier lifetime in the base region (μs)

δE_g = Shrinkage of the energy gap (eV)

ρ_c = Contact resistance ($\Omega \cdot cm^2$)

ρ_m = Metal resistivity ($\Omega \cdot cm$)

λ = Wavelength (μm)

Appendix A: Determination of the maximum operating power density (P_m) and total fraction power loss (F_{sum})

Calculations of the short-circuit current density (J_{sc}) and open circuit voltage (V_{oc}) for the maximum operating power (P_m) and the total fractional power losses (F_{sum}) from ohmic resistance losses are the essential factors to optimize a solar cell based on the geometric design parameters.

- **Calculation of short-circuit current density (J_{sc}) and open circuit voltage (V_{oc})**

The total current density (J_L) can be expressed as

$$J_L = J_E + J_{SCR} + J_B \tag{A-1}$$

where, individual value of J_E , J_{SCR} , and J_B can be refereed by the publication of Jain, Heaselll, and Roulston [9] and Singal [10].

Total current density (J_L) can be calculated as

$$J_E = qn_{ph}(1-R)\left[\frac{\alpha L_p}{{L_p}^2\alpha^2-1}\right] \times \left[\frac{\left(\left(\frac{S_pL_p}{D_p}\right)+\alpha L_p\right)-e^{-\alpha T_e}\left(\left(\frac{S_pL_p}{D_p}\right)\cosh\left(\frac{T_e}{L_p}\right)+sinh\left(\frac{T_e}{L_p}\right)\right)}{\left(\frac{S_pL_p}{D_p}\right)sinh\left(\frac{T_e}{L_p}\right)+cosh\left(\frac{T_e}{L_p}\right)} - \alpha L_p e^{-\alpha T_e}\right] \tag{A-2}$$

$$J_B = \mathrm{q}n_{ph}(1-R)\left(\frac{L_n\alpha}{{L_n}^2\alpha^2-1}e^{(-T_e+t_{scr})\alpha}\right)\times\left[L_n\alpha-\frac{\left(\frac{S_nL_n}{D_n}\right)\left[cosh\left(\frac{T_b}{L_n}\right)-e^{-\alpha T_b}\right]+sinh\left(\frac{T_b}{L_n}\right)+L_n\alpha e^{-\alpha T_b}}{\left(\frac{S_nL_n}{Dn}\right)sinh\left(\frac{T_b}{L_n}\right)+cosh\left(\frac{T_b}{L_n}\right)}\right] \quad \text{(A-3)}$$

$$J_{SCR=}\ \mathrm{q}n_{ph}(1-R)e^{-T_e\alpha}(1-e^{-t_{scr}\alpha}) \quad \text{(A-4)}$$

$$t_{scr} = \sqrt{\frac{2K_s\varepsilon_0V_{bi}}{q}\frac{(N_a+N_d)}{N_aN_d}} \quad \text{(A-5)}$$

The photon flux density $n_{ph}(\lambda)$ and Si absorption coefficient were described by Liou and Wong [11] under AM1.5 global normal sun condition can be approximated with two linear curves as

$$n_{ph}(\lambda) = C(19.7\lambda - 4.7)\times 10^{15} \qquad for\ 0.24 \le \lambda \le 0.47\ \mu\mathrm{m} \quad \text{(A-6)}$$

$$n_{ph}(\lambda) = C(-2.5\lambda + 5.7)\times 10^{15} \qquad for\ 0.48 \le \lambda \le 1.1\ \mu\mathrm{m} \quad \text{(A-7)}$$

Also, the absorption coefficient (α) of silicon material can be divided into 4 sections to obtain the data based on particular wavelength range, and is given by

$$\alpha(\lambda) = \begin{cases} 0 & for\ \lambda \ge 1.1\ \mu\mathrm{m} \\ 10^{-6.7\lambda+8.4}\ cm^{-1} & for\ 0.8 \le \lambda \le 1.1\ \mu\mathrm{m} \\ 10^{-3.3\lambda+5.6}\ cm^{-1} & for\ 0.5 \le \lambda \le 0.8\ \mu\mathrm{m} \\ 10^{-6.7\lambda+8.4}\ cm^{-1} & for\ \lambda \le 0.5\ \mu\mathrm{m} \end{cases} \quad \text{(A-8)}$$

The reverse saturation g equations, this is also known as the diode eq

$$J_{01} = q n_i^2 \left(\frac{}{N_aL_n} + \frac{}{N_dL_p}\right) \quad \text{(A-9)}$$

$$J_{02} = \frac{qn_it_{scr}}{2(\tau_n\tau_p)^2}e^{\left(\frac{\delta E_g}{2kT}\right)} \quad \text{(A-10)}$$

The short-circuit current density (J_{sc}) is due to the generation and collection of light-generated carriers and can be expressed as

$$J_{sc} = \mathrm{J}_L - \mathrm{J}_S = J_L - J_{01}\left[\left(e^{\frac{qV_{oc}}{kT}}\right)-1\right] - J_{02}\left[\left(e^{\frac{qV_{oc}}{nkT}}\right)-1\right] \quad \text{(A-11)}$$

Also, the open-circuit voltage (V_{oc}) can be found as

$$V_{oc} = \left(\frac{kT}{q}\right)\log\left(\frac{J_{sc}}{J_0}+1\right) \quad \text{(A-12)}$$

Thus, the maximum operating power at one sun (P_m) can be found as

$$P_m = J_m \times V_m \tag{A-13}$$

where the maximum current (J_m) and voltage (V_m) are given by

$$J_m = J_L\left(1 - \frac{1}{\nu+1-\log(\nu)}\right),\ V_m = V_{oc}(1 - \frac{1}{\nu}\log(\nu+1-\log(\nu)))\text{ , and }\ \nu = \frac{nkT}{q}V_{oc} \tag{A-14}$$

- **Calculation of total fractional power loss (F_{sum})**

The calculation of total fractional power loss (F_{sum}) was explained by Shabana, Saleh, and Soliman [12] and can be expressed as

$$F_{sum} = \sum_{i=1}^{n}\frac{P_{loss}}{P_{gneration}} = \sum_{i=1}^{n}\frac{\sum_{i=1}^{n}F_{sum}J_mV_m}{\sum_{i=1}^{n}J_mV_m} \tag{A-15}$$

where n is the number of individual terms of fractional power loss. While calculating the total fractional power loss (F_{sum}), the weighted fractional losses for the individual terms are calculated, with the weights being the power contributions from the respective terms.

The total fractional power loss (F_{sum}) can also be expressed in terms of the individual fractional power losses as

$$F_{sum} = F_{sr} + F_f + F_b + F_s + F_c \tag{A-16}$$

The resistance of the sheet can be expressed in a differential form as

$$\text{dR} = \left(\frac{Sheet\ resistance}{Distance\ along\ finger}\right)\text{ Distance between two fingers.} \tag{A-17}$$

Thus the power loss due to sheet resistance can be calculated as

$$P_{loss\_sheet} = \int_0^{D/2}\frac{\mathrm{J_m}^2\mathrm{L_f}^2D^2\mathrm{R_{sh}}}{\mathrm{L_f}}d_x = \frac{\mathrm{J_m}^2\mathrm{L_f}\mathrm{R_{sh}}}{24} \tag{A-18}$$

The power generated can be expressed as

$$P_{generation} = \mathrm{J_m} \times V_m\left(\mathrm{L_f} \times \frac{D}{2}\right) \tag{A-19}$$

The fractional power loss of sheet resistance (F_{sr}) is given by

$$F_{sr} = \frac{\mathrm{J_m}\mathrm{R_{sh}}\mathrm{D}^2}{12\mathrm{V_m}} \tag{A-20}$$

Under normal circumstances, the contact resistivity (R_c) can be written, using the concept of transfer length (L_T), as

$$R_c = \frac{\sqrt{R_{sh}\rho_c}}{L_c}\ coth\left(L_c\sqrt{\frac{R_{sh}}{\rho_c}}\right) = \frac{2L_T R_{sh}}{L_c}\ \cot\left(\frac{W_f}{2L_T}\right) \quad \text{(A-21)}$$

The specific contact resistance was described by Harrison and Reeves (1980) and the power loss of contact resistivity can be found as

$$P_{losss\_contact} = I^2 R_C = \left(J_m \times \frac{L_c}{2} \times \frac{D}{2}\right)^2 \left(\frac{2L_T R_{sh}}{L_c}\ \cot\left(\frac{W_f}{2L_T}\right)\right) \quad \text{(A-22)}$$

Thus, the fractional contact loss (F_c) is given by

$$F_c = \frac{J_m D}{2V_m} L_T R_{sh}\ \coth\left(\frac{W_f}{2L_T}\right) \quad \text{(A-23)}$$

The top of a solar cell has a series of arranged fingers intended to collect current. The corresponding resistive loss is given by

$$P_{generation} = J_m \times V_m\left(\frac{L_c}{2} D\right) \quad \text{(A-24)}$$

Because of symmetry, the equation is applied precisely at the midway along the length of finger to obtain

$$P_{loss\_finger} = I^2 R_f = \int_0^{\frac{L_f}{2}} \left(J_m \frac{D}{2} L_f\right)^2 \left(\frac{\rho_m}{W_f H_f}\right) d_x \quad \text{(A-25)}$$

Thus, the fractional power loss of a finger (F_f) can be expressed as

$$F_f = \frac{J_m \rho_m (L_f)^2 D}{48 V_m W_f H_f} \quad \text{(A-26)}$$

The ratio of width to thickness of a contact should be within the limits of the recommended aspect ratio, which is 0.23~0.25. Also, the fractional power loss of busbars (F_b) is given by

$$F_b = \frac{J_m \rho_m B (L_b)^2}{6 V_m H_b W_b} \quad \text{(A-27)}$$

The fractional power loss of shadowing (F_s) depends on the size and number of grid lines (N_f and N_b) because it prevents light from entering a solar cell. The fractional power loss of shadowing (F_s) is given by

$$F_s = \left(1 - \left(\frac{L_c^2 - (N_f W_f L_f + N_b W_b L_b - N_f W_f N_b W_b)}{L_c^2}\right)\right) \quad \text{(A-28)}$$